iJRASET
International Journal For Research in Applied Science and Engineering Technology

INTERNATIONAL JOURNAL FOR RESEARCH

IN APPLIED SCIENCE & ENGINEERING TECHNOLOGY

Volume: 12 **Issue:** VII **Month of publication:** July 2024

DOI: https://doi.org/10.22214/ijraset.2024.63666

www.ijraset.com

Call: 08813907089 | E-mail ID: ijraset@gmail.com

International Journal for Research in Applied Science & Engineering Technology (IJRASET)
ISSN: 2321-9653; IC Value: 45.98; SJ Impact Factor: 7.538
Volume 12 Issue VII July 2024- Available at www.ijraset.com

Green Synthesis and Characterization of Zinc Oxide Nanoparticles Using Nyctanthes arbor-tristis Plant Extracts: Assessing Photocatalytic Properties

Anil Kumar[1], Dr. Anil Kumar Shrotriya[2]
[1]*Research Scholar- Assistant Professor in Physics Govt. Bangur College Didwana, Mob. No.- 8875650773*
[2]*Research Guide- Associate Professor in Physics, S.P.S.B. Govt. College Shahpura, Rajasthan*

Abstract: ***In this work, zinc oxide (ZnO) nanoparticles are synthesised and characterised in an environmentally friendly manner, and their potential uses in photocatalytic processes is investigated. The green synthesis of ZnO nanoparticles involved the utilization of zinc nitrate hexahydrate (Zn(NO3)2·6H2O) and Nyctanthes arbor-tristis Plant Extracts. The nanoparticles were synthesized at an optimal temperature of 60 ◦C. The samples were analysed using energy-dispersive X-ray spectroscopy (EDX), Fourier-transform infrared spectroscopy (FTIR), scanning electron microscopy (SEM), X-ray diffraction (XRD), Dynamic Light Scattering(DLS) and UV-visible spectroscopy to determine their characteristics. ZnO nanoparticles were identified by a distinctive peak at 302 nm in UV-visible spectroscopy. SEM confirmed the nanoscale size and morphology of the ZnO particles. The elemental information obtained from the EDX examination showed that oxygen made up 22.2% of the atomic weight and zinc made up 45.6%. The diffractogram was indexed by XRD analysis at different angles that corresponded to ZnO nanoparticles. DLS determined the average crystalline size, which was 87.5 nm. FTIR examination revealed a distinctive signal at 1051 cm−1, suggesting that the nanoparticles contain functional groups. The produced nanoparticles had strong photocatalytic activity, especially when Methyl Blue was exposed to UV light and began to degrade. Rate constants and correlation coefficients were used to examine how the addition of ZnO nanoparticles affected the photocatalytic degradation process' kinetics. These nanoparticles were synthesised using an economical and ecologically friendly process. This work offers potential directions for further investigation and applications in the fields of nanotechnology, biosensor development, and water remediation.***

Keywords: ***Green synthesis, SEM, TEM, XRD, Nyctanthes arbor-tristis, eco-friendly, Zinc oxide nanoparticles, photocatalytic, water treatment.***

I. INTRODUCTION

Nanotechnology is a widely explored topic that has captured the interest of experts worldwide because to its unique features and tremendous potential for numerous applications (Tekade, Maheshwari, Soni, Tekade, & Chougule, 2017). Its importance is especially noticeable in fields like antibacterial technology and nanomedicine. (Eleraky, Allam, Hassan, & Omar, 2020). These remarkable creations have shown great promise in the development of biosensors. Nanomaterials possess not only a large specific surface area but also an increased surface area to volume ratio as their size, distribution, and morphology decrease (Khan, Saeed, & Khan, 2017). These exceptional physical characteristics enhance the reactivity of nanoparticles, making them highly responsive and adaptable to different applications. The chemical synthesis of nanoparticles often gives rise to several subsequent challenges. One of these challenges involves the presence of toxic chemical species that can become absorbed onto the nanoparticle surface during the synthesis process, rendering them unsuitable for biomedical applications (Fadeel & Garcia-Bennett, 2010). Additionally, conventional chemical methods tend to be expensive due to the requirement for costly chemical reducing agents (Manikam, Cheong, & Razak, 2011). Therefore, there is a pressing need for the development of a more eco-friendly synthesis method that produces nanoparticles with reduced toxicity.

Various plant parts, fungi, bacteria, and macro- and microalgae are used in green synthesis techniques to meet this need. Plant extracts are one of these methods that has a lot of promise. Plant extracts are beneficial because they are readily available, have minimal biohazard potential, and do not require cell culture procedures. (Ahmed, Annu, Chaudhry, & Ikram, 2017). Various plant parts such as roots, bark, fruits, flowers, and leaves have been employed in previous studies for the synthesis of nanoparticles.

Metal oxide nanoparticles have attracted a lot of attention because of their exceptional electrical, optical, magnetic, and catalytic characteristics (Chavali & Nikolova, 2019). These nanoparticles have special properties including surface plasmon resonance, which makes them especially useful for optical imaging.. Zinc oxide stands out among the other metal oxides as a very promising option for biomedical uses, especially in the areas of cell imaging, biosensing, antibacterial, anti-cancer, and anti-diabetes applications. Zinc oxide nanoparticles also have advantageous properties for biological material applications. They are perfect for usage in a variety of biomedical contexts since they are easily produced, non-toxic, biocompatible, and physiologically safe (Mirzaei & Darroudi, 2017).

This study uses the plant extract of Nyctanthes arbor-tristis, an Indian medicinal plant valued for its complex phytochemical profile, to create ZnO nanoparticles in a unique way. However, this study marks the first instance of utilizing the plant extract of Nyctanthes arbor-tristis, for the formulation of Zinc oxide nanoparticles.

Excellent photocatalytic activity is demonstrated by zinc nanoparticles (ZnO NPs) in the breakdown of dyes. Zinc oxide nanoparticles (ZnO NPs) were prepared in this study using a green synthesis approach. These NPs were then characterised using various analysis techniques, including ultraviolet-visible (UV-vis), Fourier-transform infrared (FTIR), X-ray diffraction (XRD), dynamic light scattering (DLS), and transmission electron microscopy (TEM). Under visible light, the synthesised ZnO NPs showed efficient photocatalytic activity for degrading dyes. In particular, the effectiveness of the synthesised ZnO NPs was assessed by looking at the photocatalytic degradation of Methylene Blue dye.

Reagents: Zinc nitrate hexahydrate and methylene blue were purchased from CDH and Sigma Aldrich respectively. DI water was taken from Organo biotech private limited. Leaves of *Nyctanthes arbor-tristis* plant were collected from nearby garden. Whatman filter paper grade no. 1 size 125 mm was purchased from local vendor.

II. INSTRUMENTS

Using the Shimadzu IRAffinity-1S model in Attenuated Total Reflectance (ATR) mode, Fourier Transform Infrared Spectroscopy (FTIR) was carried out over a 4000-400 cm-1 spectral range. The FTIR analysis was conducted at a resolution of 8 cm^{-1} with a scanning speed of 64 scans/min. The Shimadzu UV 1900i model was used to record UV-Visible (UV-Vis) spectroscopy for the analysis of nanoparticle production. The particle size distribution of the nanoparticles was determined via Dynamic Light Scattering (DLS) spectroscopy, employing the Litesizer 500 model from Anton Paar. The morphological patterns and elemental composition of the synthesized samples were assessed using a Field Emission Scanning Electron Microscope (FESEM), operated at an energy setting of 10 KeV (Zeiss Supra 55VP, EDAX Ametek). Prior to imaging, the samples were mounted on carbon adhesive tape affixed to an aluminum stage and sputter-coated with gold using an Emitech K550X sputter coater from Labtech International for 120 seconds. The size and morphology of the synthesized nanoparticles were further characterized using Transmission Electron Microscopy (TEM) with a Jeol Jem-1400 model. The crystalline nature of the synthesized nanoparticles was determined by X-Ray Diffraction (XRD) using a Rigaku Ultima IV model, scanning from 5 to 60 degrees at a rate of 2 degrees/min with a CuKα radiation source.

III. EXPERIMENTAL

A. Preparation of Leaf Extract

Leaf extract from *Nyctanthes arbor-tristis* (commonly known as night-flowering jasmine) was prepared for the synthesis of nanoparticles. Fresh leaves of N. arbor-tristis were collected, thoroughly washed with deionized water to remove any surface contaminants, and then air-dried. Subsequently, 20 grams of the clean leaves were cut into small pieces and immersed in 100 milliliters of deionized water. This mixture was heated to 60°C and maintained at this temperature for 1 hour, during which the solution gradually turned a light green color, indicating the release of phytochemicals into the aqueous medium. The resultant leaf extract was then filtered through Whatman No. 1 filter paper to remove any solid plant residues, and the filtrate was collected for subsequent nanoparticle synthesis.

B. Synthesis of ZnO nanoparticles

Zinc oxide (ZnO) nanoparticles were synthesized using zinc nitrate hexahydrate (Zn(NO3)2·6H2O) as a precursor. A 0.1 M solution of Zn(NO3)2·6H2O was prepared by dissolving the requisite amount in 10 mL of deionized water. Three different sets of reactions were carried out by varying the volume of Nyctanthes arbor-tristis leaf extract added to the zinc nitrate solution. Specifically, 1 mL, 3 mL, and 6 mL of the prepared leaf extract were added dropwise to the zinc nitrate solution under continuous magnetic stirring at 60°C. The stirring was maintained for 24 hours to ensure thorough mixing and facilitate the formation of ZnO nanoparticles. During the reaction, the solution color changed from colorless to light brown, indicating the formation of ZnO nanoparticles.

IV. RESULTS AND DISCUSSION

A. *UV-Vis Spectroscopy*

The UV-Vis absorption spectra of ZnO nanoparticles displayed a distinct peak around 302 nm (Figure 1) (Amuthavalli, et al., 2021) (Arefi & Rezaei-Zarchi, 2012) (Singh, Pandey, Yadav, & Singh, 2013). This peak corresponded to the characteristic absorption band of ZnO nanoparticles. The absorption at this wavelength is typically associated with the electronic transitions from the valence band to the conduction band of ZnO. The presence of this peak highlighted the strong UV light absorption capability of ZnO nanoparticles, which is crucial for their photocatalytic activities.

The UV-Vis spectroscopy data further revealed that the intensity of the absorption band around 302 nm increased with higher concentrations of leaf extract. Notably, ZnO-3, synthesized using 6 mL of leaf extract, exhibited the highest intensity at this wavelength, indicating a more complete transformation of the precursor into ZnO nanoparticles. In contrast, ZnO-1, which was synthesized with only 1 mL of leaf extract, showed a very low intensity band at 302 nm, suggesting a significantly lower degree of precursor conversion. These observations underscore the critical role of the leaf extract concentration in the synthesis process, where higher amounts of the reducing agent facilitate a more effective and complete formation of ZnO nanoparticles.

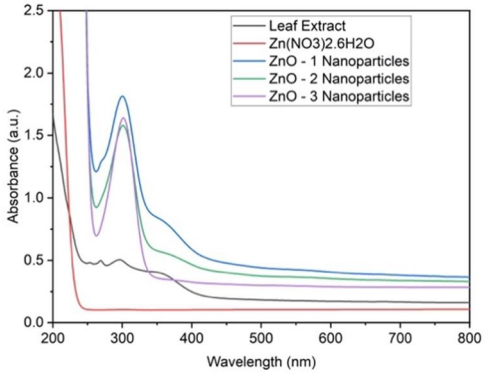

Figure 1. UV-Vis spectra of ZnO nanoparticles at different concentrations of leaf extract.

B. *Dynamic Light Scattering*

The size of the synthesized nanoparticles was measured using Dynamic Light Scattering (DLS), as shown in Figures 2A-2C. The graphs indicated that ZnO nanoparticles synthesized from Zn(NO3)2·6H2O showed average sizes of 224.8 nm, 135.9 nm, and 87.5 nm for ZnO-1, ZnO-2, and ZnO-3, respectively. The size decreased as the leaf extract concentration increased from 1 mL to 6 mL. These results collectively demonstrate that increasing the concentration of the reducing and capping agent effectively reduces the size of the nanoparticles, confirming the influence of synthesis conditions on nanoparticle dimensions.

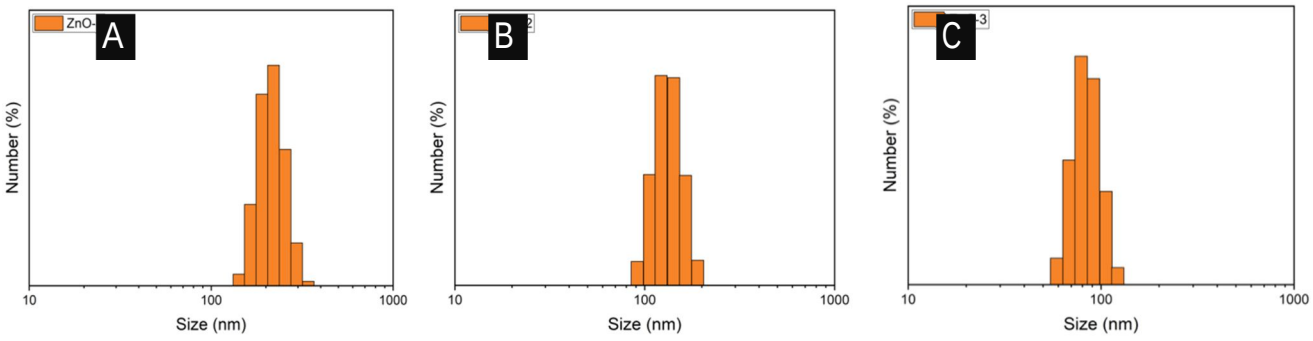

Figure 2. DLS spectra of (A) ZnO-1, (B) ZnO-2, and (C) ZnO-3 nanoparticles at different concentrations of leaf extract.

C. *X-Ray Diffraction*

The crystalline structure of ZnO nanoparticles synthesized from Zn(NO3)2·6H2O as a precursor was analyzed using X-ray diffraction (XRD), as shown in Figure 3. The sample ZnO-3 was chosen for further characterization and application as it showed the smallest size. The crystalline structure of synthesized ZnO nanoparticles were investigated through XRD as shown in Figure 3.The XRD analysis of the synthesized ZnO nanoparticles, as presented in the resulting pattern, showed distinct peaks at 2θ values of 31.30°, 33.98°, 36.08°, 47.24°, 57.03°, 63.18°, and 67.79°.

These peaks correspond to the crystallographic planes (100), (002), (101), (102), (110), (103), and (112), respectively. The diffraction pattern closely matched the standard JCPDS card no. 36-1451 (Mohammad Reza Arefi & Rezaei-Zarchi, 2012), confirming that the ZnO nanoparticles possess a wurtzite phase with a hexagonal crystalline structure, specifically within the P63mc space group. Additionally, the absence of any peaks associated with impurities indicates that the synthesized ZnO nanoparticles are of high purity.

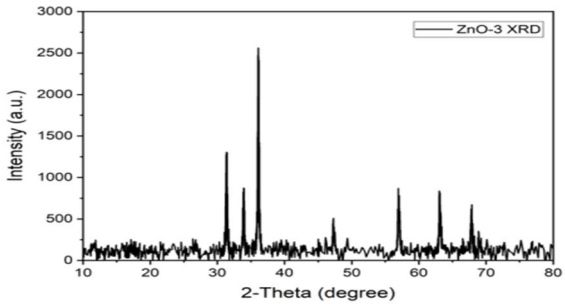

Figure 3. XRD graphs ZnO-3 nanoparticles.

D. Fourier Transform Infrared Spectroscopy

The formation of MnO2 and ZnO nanoparticles were confirmed by FTIR in ATR mode. The leaf extract and the salt precursor were also characterized via FTIR. The Figure 4 depicted the FTIR spectra of ZnO nanoparticles synthesized from Zn(NO3)2·6H2O as precursor. The leaf extract spectra showed band at ~3300 cm^{-1} arising from OH stretching vibrations due to the presence of various different types of flavonoids in the leaf extract. The spectra in Figure 4 represented the ZnO nanoparticles synthesized from zinc nitrate hexahydrate. In the nanoparticle spectra, the intensity of the bands at ~3300 $cm^{-1}$and ~1635 cm^{-1}increased due to the presence of leaf extract in the nanoparticle samples. However, a new band at ~1051 cm^{-1}confirmed the reduction of zinc salt into zinc oxide nanoparticles.

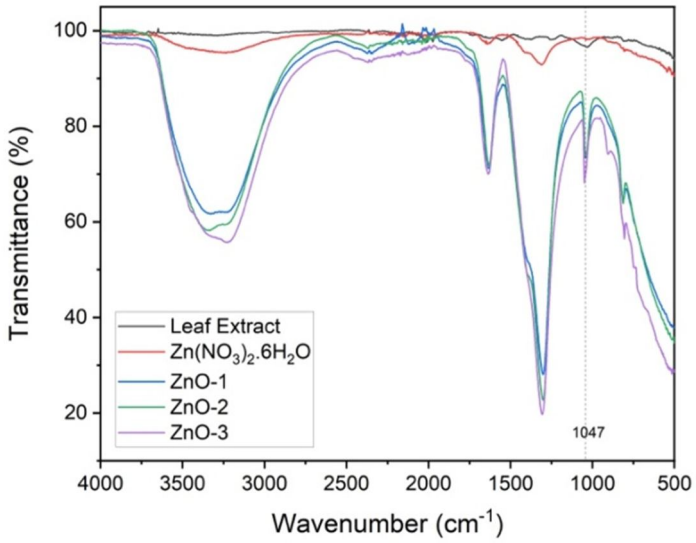

Figure 4. ATR-FTIR spectra of ZnO nanoparticles respectively at different concentrations of leaf extract.

E. Scanning Electron Microscopy and EDAX

In this analysis, the ZnO-3 nanoparticle were synthesized and subjected to Scanning Electron Microscopy (SEM) coupled with Energy Dispersive X-ray Spectroscopy (EDS) to ascertain their morphological and elemental composition characteristics. The SEM image of ZnO-3 (Figure 5A) reveals its surface morphology, while the corresponding EDS elemental mapping (Figures 5B-E) and composition table (Figure 5F) indicate the presence carbon (32.2%), oxygen (22.2%), and zinc (45.6%). These compositional analyses not only corroborate the successful synthesis of the targeted materials but also provide critical insights into their elemental distribution, essential for understanding their potential applications in various domains.

ISSN: 2321-9653; IC Value: 45.98; SJ Impact Factor: 7.538
Volume 12 Issue VII July 2024- Available at www.ijraset.com

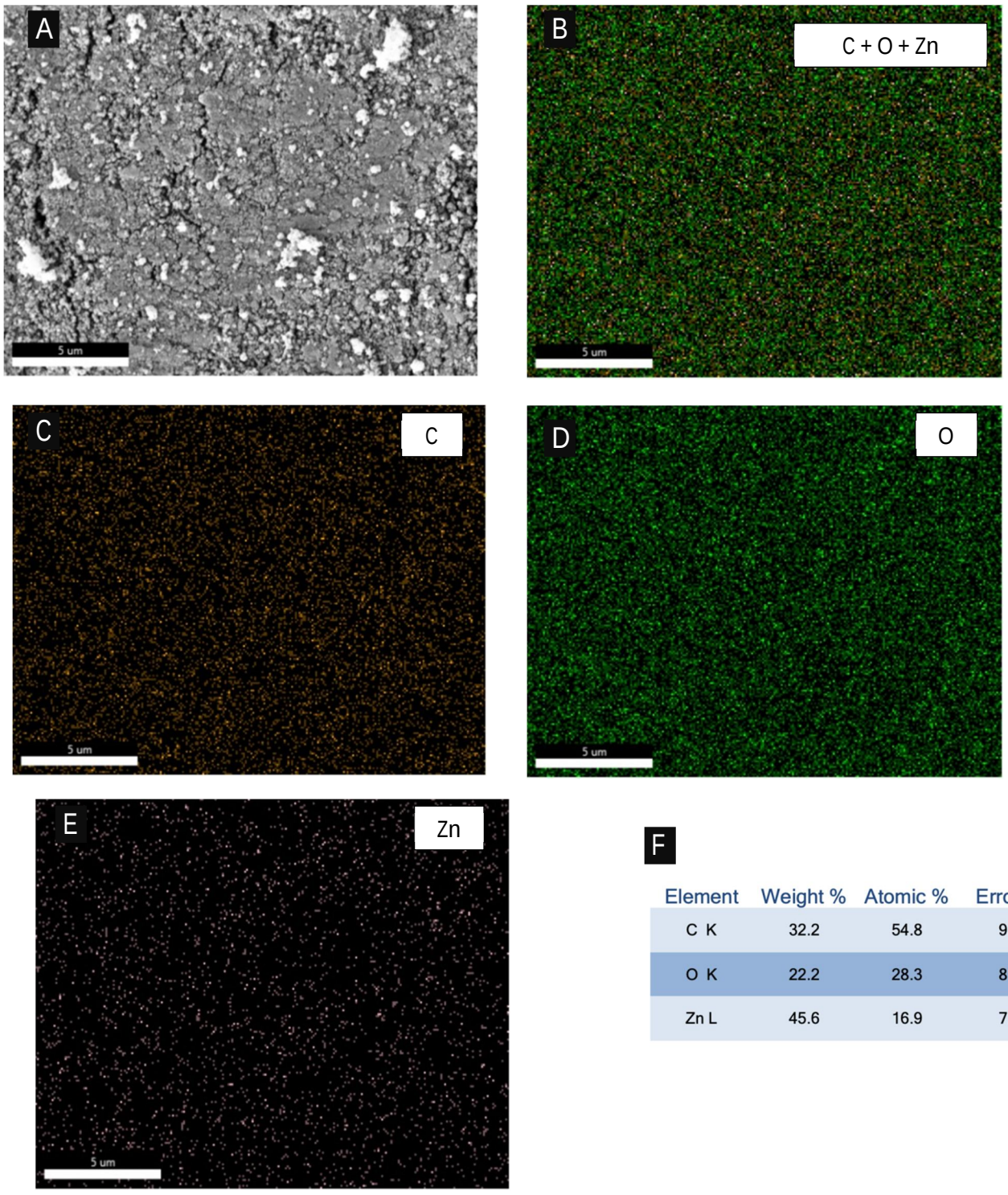

F

Element	Weight %	Atomic %	Error %
C K	32.2	54.8	9.2
O K	22.2	28.3	8.2
Zn L	45.6	16.9	7.4

Figure 5. (A)SEM image of ZnO-3 nanoparticles (B) Overall elemental mapping with individual elemental mapping of (C) carbon, (D) oxygen, and (E) zinc element along with (F) composition table.

F. Transmission Electron Microscopy and Size Distribution

Figure 6 presents the Transmission Electron Microscopy (TEM) images and corresponding particle size distribution graphs for ZnO-3 nanoparticles. The TEM image of ZnO-3 nanoparticles (Figure 6A) also exhibit a spherical shape, with a particle size of 85±15 nm as illustrated in Figure 6B. These TEM analyses confirm the uniformity in shape and provide precise measurements of the nanoparticle sizes, critical for their application in various nanotechnological and industrial fields.

ISSN: 2321-9653; IC Value: 45.98; SJ Impact Factor: 7.538
Volume 12 Issue VII July 2024- Available at www.ijraset.com

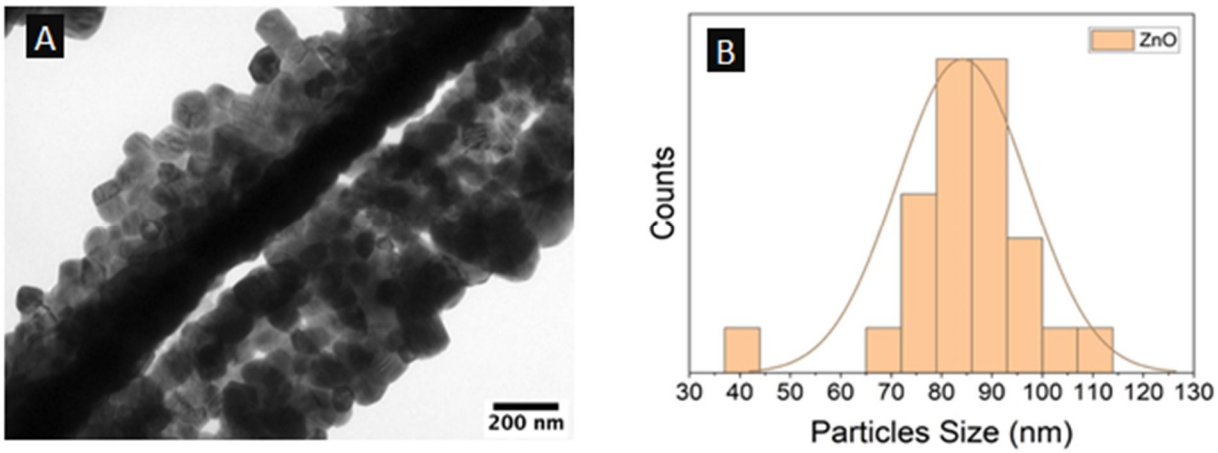

Figure 6. Showing the TEM images (A) Morphology of ZnO-3 nanoparticles and its (B) particle size distribution graph.

V. PHOTOCATALYTIC ACTIVITY OF NANOPARTICLES

A. Visual observation and UV-Vis study

The purpose of the study was to examine how ZnO-3 nanoparticles degraded Methylene Blue (MB) dye and assess their photocatalytic efficacy in direct sunshine over a range of time periods. The photodegradation of MB dye was observed using UV-Vis spectroscopy in addition to visual inspection.Initially, the MB solution, with a starting concentration of 10 mg/L, exhibited a distinct blue colorat the zero-minute mark after the introduction of ZnO-3 nanoparticles as illustrated in Figure7. The solution's blue colour started to fade over time, signifying the dye's gradual degradation. The solution turned practically colourless after being exposed to direct sunshine for 360 minutes, indicating significant MB dye degradation. This finding implies that under sun light, the ZnO-3 nanoparticles efficiently assisted the dye's photocatalytic breakdown.

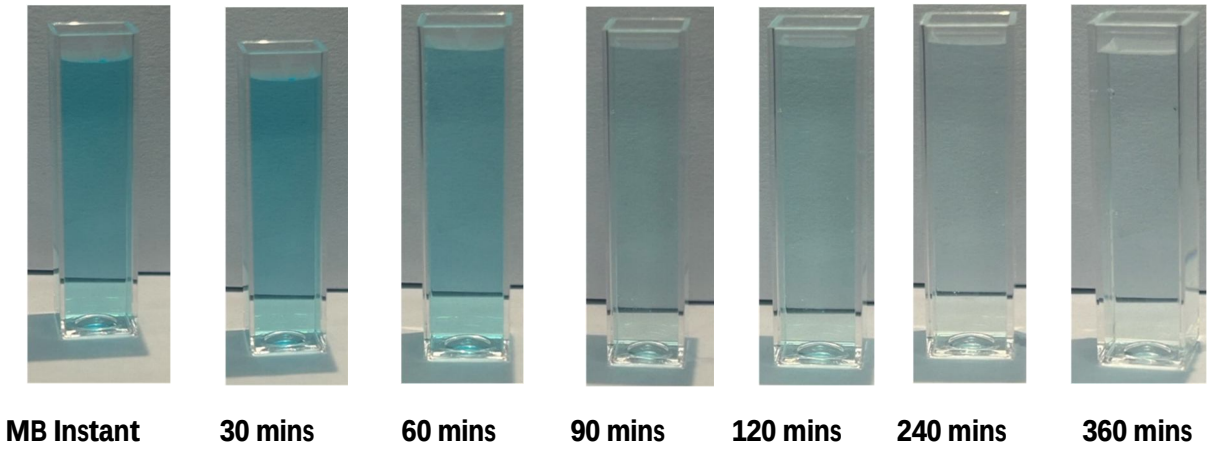

Figure 7. Visual observation of the photocatalytic degradation of MB dye ZnO-3 nanoparticles.

However, UV-Vis spectroscopy was used to calculate the photocatalytic efficiency. Using a UV-Vis absorption spectrometer, the characteristic absorption peak of Methylene Blue (MB) was detected at a maximum wavelength (λmax) of roughly 664 nm, which is an important marker for monitoring dye degradation. Before the MB solution was exposed to sunlight, its initial absorbance was measured. From then on, measurements were made at regular intervals to track changes over time. By maintaining a constant dye concentration of 10 mg/L and a fixed nanoparticle dose of 5 mL, the study assessed the impact of contact time on the photocatalytic degradation of MB dye at various intervals (0, 30, 60, 90, 120, 180, 240, and 360 minutes). The maximum absorption wavelength did not vary over the degrading process, however the MB absorption peaks' intensity gradually dropped. Figures 8A demonstrate the considerable dye degradation suggested by this trend. Furthermore, graphs showing the percentage of degradation in relation to absorbance intensity over time were generated (Figures 8B). The greatest photodegradation efficiency for ZnO-3 nanoparticles was measured at 66.51% after 360 minutes of exposure to direct sunshine.

The dye degradation was rather moderate at first, reaching about 24% for ZnO-3 nanoparticles up to 120 minutes. On the other hand, the degradation rate quickened as the contact duration grew, reaching its maximum values after 360 minutes. The increased deterioration over longer contact durations emphasises how crucial continuous exposure is to successful photocatalytic activity.

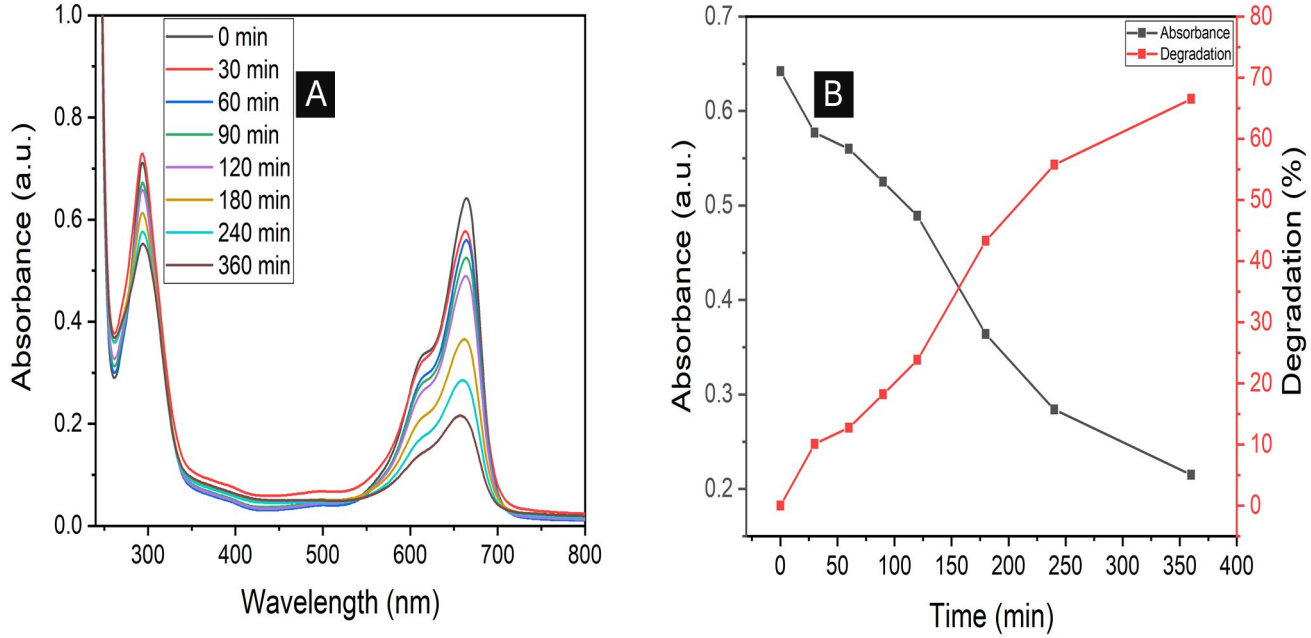

Figure 8(A) Absorbance spectra, (B) Effect of time on degradation percentage by ZnO-3 nanoparticles.

VI. RESULT AND DISCUSSION

A. Kinetic study of dye degradation

The produced nanoparticles' decomposition of Methylene Blue (MB) followed the pseudo-first-order kinetics kinetic model, which is based on a modified Langmuir-Hinshelwood technique (kumar, thakur, kumar, & jeet, 2023) (Abu-Dief, Essawy, diab, & mohamed, 2021) (Hashemi, Poursalehi, & Delavari, 2022).

$$ln\ \frac{C}{C_0} = -kt$$

where, Co and C are the initial and final concentration of Mb dye in the solution, k is the rate constant, and t is the contact time.
The above equation can be adapted accordingly (Goudjil, Dali, Zighmi, Mahcene, & Bencheikh, 2024) as shown below:

$$ln\ \frac{A}{A_0} = -kt$$

Here, the dye's initial concentration is shown by the letter C_0, and the associated absorbance value is shown by the letter A_0. The dye concentration is shown as C after irradiation, and the matching absorbance value is shown as A. The data was plotted for ln (A/A_0) versus time, as shown in 9A. A good linear fit was obtained by applying the first-order kinetics principle, as shown in Figures 9B, with regression coefficients of 0.967 for ZnO-3 nanoparticles. For ZnO-3 nanoparticles, the estimated rate constants for the photodegradation process were found to be 0.00344 per minute. The maximum effectiveness for MB dye degradation is exhibited by ZnO-3 nanoparticles, as further validated by these rate constants. Zinc nitrate hexahydrate was used as the precursor throughout the synthesis process, which produced the lowest sized nanoparticles and is responsible for the increased efficiency of ZnO-3 nanoparticles. When these nanoparticles were exposed to direct sunlight, their smaller size enhanced the surface area available for adsorption sites, which promoted the generation of free radicals.. Because these free radicals are more likely to interact with MB dye molecules, they may be responsible for the highest degradation that has been seen (kalaycioglu, uysal, pekcan, & erim, 2023).

To sum up, the pseudo-first-order kinetics model offered a solid foundation for comprehending how ZnO-3 nanoparticles photodegraded MB dye. The variations in degradation efficiencies and rate constants brought to light how important surface area and particle size are for increasing photocatalytic activity in the presence of sunshine.

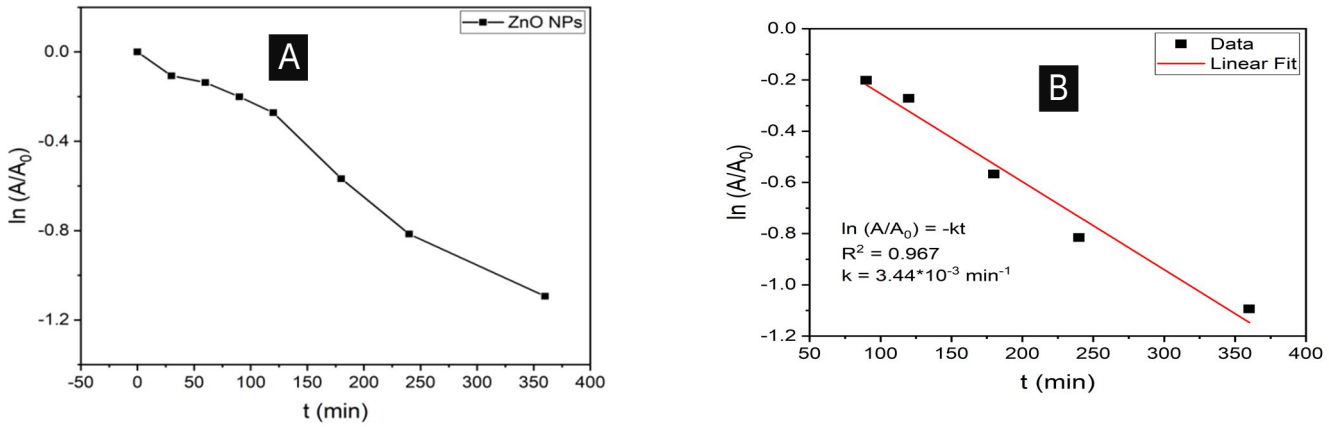

Figure 9. (A) Kinetic measurement of MB dye photodegradation, (B) Linear fitting model of kinetic measurement by ZnO-3 nanoparticles.

VII. CONCLUSION

Nyctanthes arbor-tristis leaf extract was used to successfully synthesise ZnO nanoparticles (NPs). The photocatalytic capabilities of Nyctanthes arbor-tristis were demonstrated by the green synthesis method used in this investigation. To verify the existence of MnO2 NPs, a number of characterization methods were used, including UV-vis, FTIR, XRD, DLS, TEM, and FESEM samples. The presence of ZnO NPs with an average size of roughly 87.5 nm was verified by the XRD examination. The degradation of the organic dye methylene blue was used to gauge the photocatalytic activity of the ZnO NPs, and the results indicated promising performance in this regard. The synthesis process based on plant extracts provides a workable, straightforward, economical, dependable, and eco-friendly method. To sum up, this work makes a significant contribution to the creation of ZnO NPs.

REFERENCES

[1] Tekade, R. K., Maheshwari, R., Soni, N., Tekade, M., & Chougule, M. B. (2017). Nanotechnology for the development of nanomedicine. In Nanotechnology-based approaches for targeting and delivery of drugs and genes (pp. 3-61). Academic Press.
[2] Eleraky, N. E., Allam, A., Hassan, S. B., & Omar, M. M. (2020). Nanomedicine fight against antibacterial resistance: an overview of the recent pharmaceutical innovations. Pharmaceutics, 12(2), 142.
[3] Khan, I., Saeed, K., & Khan, I. (2019). Nanoparticles: Properties, applications and toxicities. Arabian journal of chemistry, 12(7), 908-931.
[4] Fadeel, B., & Garcia-Bennett, A. E. (2010). Better safe than sorry: Understanding the toxicological properties of inorganic nanoparticles manufactured for biomedical applications. Advanced drug delivery reviews, 62(3), 362-374.
[5] Manikam, V. R., Cheong, K. Y., & Razak, K. A. (2011). Chemical reduction methods for synthesizing Ag and Al nanoparticles and their respective nanoalloys. Materials Science and Engineering: B, 176(3), 187-203.
[6] Ahmed, S., Ahmad, M., Swami, B. L., & Ikram, S. (2016). A review on plants extract mediated synthesis of silver nanoparticles for antimicrobial applications: a green expertise. Journal of advanced research, 7(1), 17-28.
[7] Chavali, M. S., & Nikolova, M. P. (2019). Metal oxide nanoparticles and their applications in nanotechnology. SN applied sciences, 1(6), 607.
[8] Mirzaei, H., & Darroudi, M. (2017). Zinc oxide nanoparticles: Biological synthesis and biomedical applications. Ceramics International, 43(1), 907-914.
[9] Amuthavalli, P., Hwang, J. S., Dahms, H. U., Wang, L., Anitha, J., Vasanthakumaran, M., ... & Singh, S. (2021). Zinc oxide nanoparticles using plant Lawsonia inermis and their mosquitocidal, antimicrobial, anticancer applications showing moderate side effects. Scientific reports, 11(1), 8837.
[10] Arefi, M. R., & Rezaei-Zarchi, S. (2012). Synthesis of zinc oxide nanoparticles and their effect on the compressive strength and setting time of self-compacted concrete paste as cementitious composites. International journal of molecular sciences, 13(4), 4340-4350.
[11] Singh, D. K., Pandey, D. K., Yadav, R. R., & Singh, D. (2013). A study of ZnO nanoparticles and ZnO-EG nanofluid. Journal of Experimental Nanoscience, 8(5), 731-741.
[12] Kumar, P., Thakur, N., Kumar, K., & Jeet, K. (2023). Photodegradation of methyl orange dye by using Azadirachta indica and chemically mediated synthesized cobalt doped α-Fe2O3 NPs through co-precipitation method. Materials Today: Proceedings.
[13] Abu-Dief, A. M., Essawy, A. A., Diab, A. K., & Mohamed, W. S. (2021). Facile synthesis and characterization of novel Gd2O3–CdO binary mixed oxide nanocomposites of highly photocatalytic activity for wastewater remediation under solar illumination. Journal of Physics and Chemistry of Solids, 148, 109666.
[14] Hashemi, E., Poursalehi, R., & Delavari, H. (2022). Structural, optical and photocatalytic activity of multi-heterojunction Bi2O3/Bi2O2CO3/(BiO) 4CO3 (OH) 2 nanoflakes synthesized via submerged DC electrical discharge in urea solution. Nanoscale Research Letters, 17(1), 75.
[15] Goudjil, M. B., Dali, H., Zighmi, S., Mahcene, Z., & Bencheikh, S. E. (2024). Photocatalytic degradation of methylene blue dye with biosynthesized Hematite α-Fe2O3 nanoparticles under UV-Irradiation. Desalination and Water Treatment, 317, 100079.
[16] Kalaycıoğlu, Z., Özuğur Uysal, B., Pekcan, O., & Erim, F. B. (2023). Efficient photocatalytic degradation of methylene blue dye from aqueous solution with cerium oxide nanoparticles and graphene oxide-doped polyacrylamide. ACS omega, 8(14), 13004-13015.

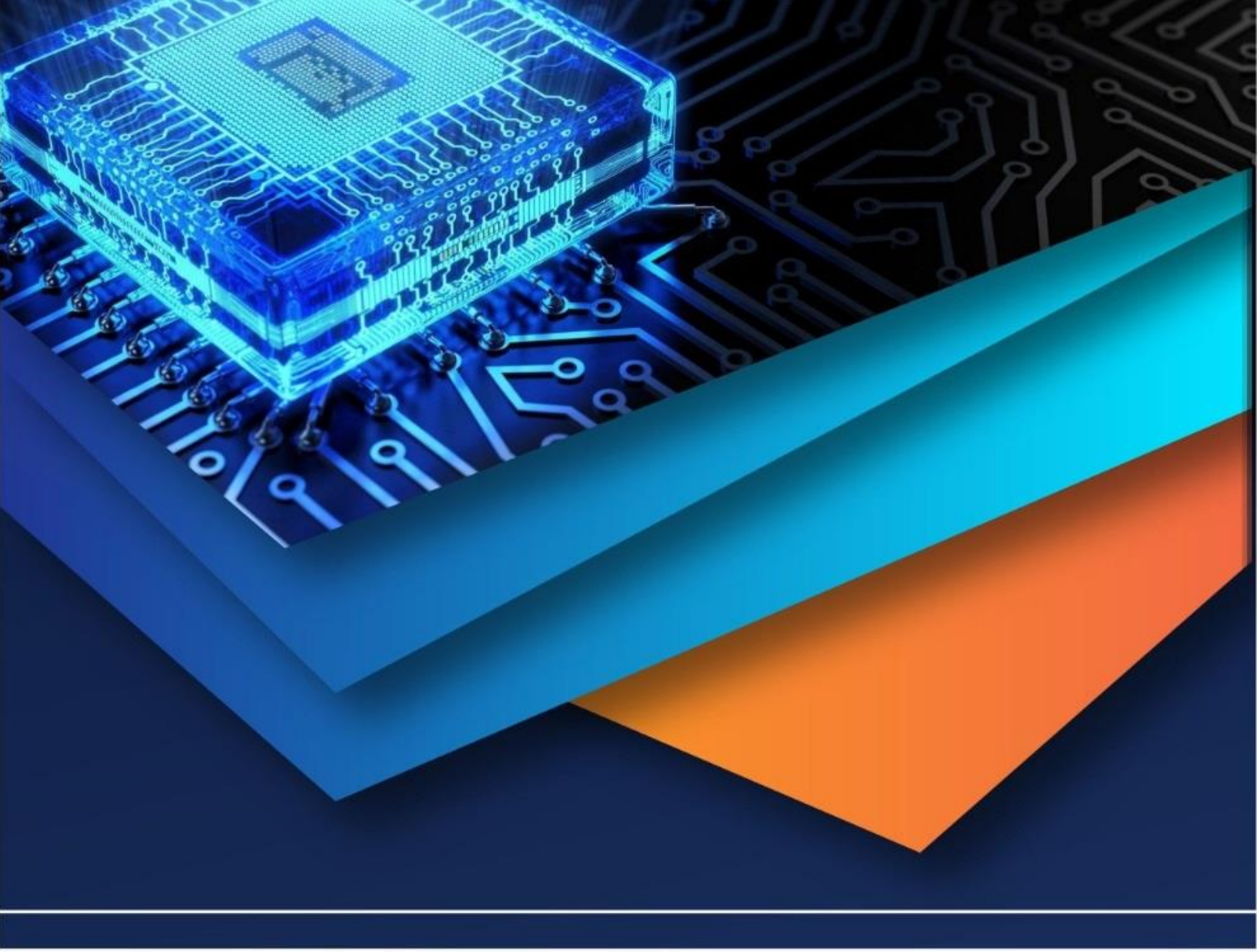

10.22214/IJRASET

45.98

IMPACT FACTOR: 7.129

IMPACT FACTOR: 7.429

INTERNATIONAL JOURNAL FOR RESEARCH

IN APPLIED SCIENCE & ENGINEERING TECHNOLOGY